International Journal of Mass Spectrometry 276 (2008) 102–109

Contents lists available at ScienceDirect

International Journal of Mass Spectrometry

journal homepage: www.elsevier.com/locate/ijms

Charge inversion of polypeptide anions using protein and dendrimer cations as charge inversion reagents☆

Joshua F. Emory, Scott A. McLuckey*

Department of Chemistry, Purdue University, 560 Oval Drive, West Lafayette, IN 47907-2084, United States

ARTICLE INFO

Article history:
Received 7 February 2008
Received in revised form 17 April 2008
Accepted 21 April 2008
Available online 1 May 2008

Keywords:
Charge inversion
Ion/ion reaction
Linear ion trap
Peptide mixture

ABSTRACT

The conversion of deprotonated bradykinin, as well as anions derived from other polypeptides, to protonated species has been demonstrated via ion/ion reactions with multiply protonated polypropylenimine diaminobutane (DAB) dendrimers and proteins in a linear ion trap. The charge inversion characteristics of both the proteins and the dendrimers were examined with emphasis on the extent of charging of the analyte and the tendency for adduct formation. Multiply protonated proteins, for example, tended to result in significant adduct formation whereas the multiply protonated amino-terminated dendrimers showed essentially no adduct formation. Ions derived from five dendrimer generations were examined as charge inversion reagents with deprotonated bradykinin serving as a peptide model. Both the size and the charge state of the dendrimer reagent ion played a role in determining the number of protons transferred from the reagent cation to the peptide anion. For a given dendrimer generation, the tendency is for increasing numbers of protons to transfer with increasing dendrimer charge. For a given charge state, the numbers of protons transferred tends to be inversely related to dendrimer size. All of the observed data are consistent with charge inversion taking place via a long-lived intermediate complex with the ultimate products being determined by the fate of the complex (i.e., stabilization of the complex versus break-up into one of several competitive dissociation channels).

1. Introduction

Mass spectrometry has come to play a central role in the identification and characterization of proteins. In the frequently encountered cases in which mixtures of peptides or proteins are present, tandem mass spectrometry is routinely performed to obtain structural information. The quality and quantity of structural information that can be obtained with a tandem mass spectrometry experiment is largely dependent upon the gas-phase ion chemistry of the peptide or protein ions that takes place between stages of mass analysis. Ionization is essential to any mass spectrometry application and the two principle ionization methods that are most commonly used to generate large peptide and protein ions are matrix-assisted laser desorption ionization (MALDI) [1,2] and electrospray ionization (ESI) [3]. In the positive ion mode, MALDI typically yields primarily singly protonated molecules, in some cases along with some multiply protonated molecules of lower abundance. The formation of primarily singly charged ions facilitates mixture analysis in single stage mass spectrometry because it avoids charge state ambiguity, but singly charged protein ions tend to provide limited structural information upon interrogation by commonly used gas-phase dissociation methods. In part for this reason, MALDI is not as widely used as ESI as an ionization method for tandem mass spectrometry of proteins. ESI typically forms multiply charged ions of peptides and proteins, and usually provides a distribution of charge states from molecules that are capable of accommodating multiple charges. Previous studies have shown that gas-phase fragmentation can be highly sensitive to parent ion charge state [4–8] and that complementary structural information can be obtained from dissociation of ions of different charge states, highlighting the significance of controlling the charge states of macro-ions [9].

The charge state manipulation of macro-ions formed by ESI has been effected by several methods including manipulation of solution conditions [10], and the use of either ion/molecule or ion/ion chemistry to reduce ion charge in the gas-phase [11–14]. Ion/ion reactions have proven to be particularly well suited for charge state manipulation of gas-phase ions [11–13,15–17]. The highly exothermic nature of virtually all ion/ion reactions makes them efficient in reducing charge states of macro-ions to arbitrarily low values [18]. Care must be taken to choose reagents that avoid the formation of reagent–analyte complexes, which also may be observed with ion/molecule reactions intended to lead to

☆ Prepared for Special Issue of IJMS on Ion/Electron and Ion/Ion Interactions.

* Corresponding author. Tel.: +1 765 494 5270; fax: +1 765 494 0239.
E-mail address: mcluckey@purdue.edu (S.A. McLuckey).

1387-3806/$ – see front matter © 2008 Published by Elsevier B.V.
doi:10.1016/j.ijms.2008.04.013

proton transfer [18,19]. Most detailed studies of ion/ion reactions have been conducted via ion trap tandem mass spectrometry. A number of analytically useful measurements involving protein ion charge state manipulation within ion traps has been demonstrated [5–7,20], which include the use of ion/ion reactions to simplify mass spectra of protein mixtures [6,21,22], to simplify protein product ion spectra derived from multiply charged ions [5,6,23,24], to concentrate ions into a single charge state [25], and to dissociate multiply charged ions via electron-transfer dissociation (ETD) [26,27].

Most ion/ion reactions have emphasized the use of singly charged reagent ions that give rise to either single proton or single electron transfer. The reduction of a protein's charge state by more than one charge can be achieved via sequential ion/ion reactions. However, sequential single charge transfer reactions are not suitable for changing the polarity of a protein ion. Previous methods for changing ion polarity in the gas-phase include ion/neutral collisions, generally conducted at kiloelectron-volt collision energies, involving electronic transitions [28,29]. Product ions of these reactions are often formed in excited electronic states, which often results in extensive fragmentation [28,30,31]. Ion/ion reactions at low relative translational energies provide an alternative to ion/neutral collisions at high translational energies for charge inversion. In addition, ion/ion reactions have cross-sections orders of magnitude larger than those of the endothermic reactions associated with the high-energy beam experiments with little or no fragmentation being observed in ion/ion reactions, when appropriate conditions are used. Ion/ion charge inversion reactions have high enough efficiencies to allow sequential charge inversion reactions (i.e., positive to negative-to-positive and vice versa) to be conducted with overall efficiencies on the order of tens of percent [32,33]. The negative-to-positive charge inversion efficiency, which is defined as the fraction of anions of the analyte undergoing ion/ion reactions that are converted to cations, is highly dependent on the chemical and physical properties of the charge inversion reagent used.

A charge inversion step enables ion formation in one polarity and analysis in the opposite polarity mode. It has been observed that fragmentation of ions of opposite polarity can provide complementary structural information [34]. Interrogating protein or peptide ions of both polarities is seldom performed, however, even when potentially valuable information might be obtained, presumably due to the additional time and experimental effort associated with analysis of the sample in both polarities. The ability to manipulate ion charge states and polarities independent of a fixed set of ionization conditions would facilitate access to the complementary structural information available from both ion polarities. For instance, negative-to-positive charge inversion would allow for acquisition of collision-induced dissociation (CID) data from positive ions, which often give more informative dissociation data than negative ions. Other dissociation techniques such as ETD also work more efficiently on multiply positively charged ions and charge inversion of a negative ion to a multiply charged positive ion enables analyte interrogation via ETD. The utility of this approach was demonstrated through the charge inversion of a negative phosphopeptide ion to a doubly positively charged phosphopeptide ion followed by ETD analysis [35]. Recently, negative-to-positive and positive to negative charge inversion of bradykinin has been performed using multiply charged dendrimer ions as charge inversion reagents [9,36]. In the positive to negative charge inversion case, ubiquitin ion charge was inverted using both dendrimer anions and smaller organic anions. In the current study, we systematically investigate the merits of proteins and dendrimers as negative-to-positive charge inversion reagents via reactions with singly deprotonated peptides.

2. Experimental

Positive protein ions were formed via electrospray from a ~2% (v) aqueous acetic acid solution of ~50–100 μM concentration. Negative peptide ions were formed via electrospray from a ~50–100 μM aqueous solution of ~2–5% (v) ammonium hydroxide. The peptide mixture solution containing GAILXGAILR [X = the amino acids D/K/P] and KGAILXGAILR [X = the amino acids A/P/D/K] and the bradykinin solution were electrosprayed from methanol/H_2O (50/50, v/v) with ~2–5% ammonium hydroxide. Diaminobutane (DAB) dendrimers were subjected to electrospray from a ~2% acetic acid aqueous solution with a dendrimer concentration between ~1–2% by weight. Bovine cytochrome *c*, bovine insulin, bradykinin, and the DAB dendrimers were purchased from Sigma (St. Louis, MO), while the GAILXGAILR and KGAILXGAILR peptides were obtained from SynPep Corp. (Dublin, CA).

The charge inversion experiments using DAB dendrimer generations 1–5 as sources of reagent ions for charge inversion experiments of bradykinin −1 were performed on a Finnigan-ITMS quadrupole ion trap mass spectrometer, which is equipped with four homebuilt ion sources that included two electrospray sources and two glow discharge sources [37]. This four-source 3D ion trap instrument allowed for sequential injection and reaction of oppositely charged ions formed via electrospray. All experiments were controlled by ICMS software [38], and the negative ions were accumulated in the ion trap followed by multiple resonance ejections steps [39] to isolate a single charge state before the introduction of the positive ions leading to the charge inversion reaction. A mutual storage period of typically 100–300 ms allowed ions of opposite polarities to react before mass analysis was performed by resonance ejection [40]. Finally, experiments involving the reactions between bradykinin and DAB dendrimer generations 3, 4, and 5 were repeated on a modified MDS Sciex 2000 QTRAP (a hybrid triple quadrupole/linear ion trap instrument) [41] taking advantage of its superior ability to isolate both the reagent ion and the analyte ion prior to the ion/ion reaction. Both the reagent and analyte ions were selected by the mass-resolving quadrupole (Q1) and accumulated in the collision cell (Q2), which was operated as a linear ion trap. After a mutual ion storage period of 100–300 ms, cations were transferred to the Q3 linear ion trap for subsequent mass analysis via mass selective axial ejection [41]. Charge inversion reactions involving the GAILXGAILR and KGAILXGAILR peptide mixture with the DAB dendrimers were performed with an MDS Sciex 4000 QTRAP, which was modified similarly to the 2000 QTRAP for ion/ion reactions. This instrument was used simply because it was available and not because of any fundamental differences in the abilities of the two different models of QTRAP for executing experiments of this type. In this case, the reagent ions were isolated prior to the ion/ion reaction whereas the mixture of peptide analyte ions was admitted with Q1 operated in RF-only mode. All spectra shown here represent an average of 20–100 scans and in all the spectra that are directly compared, as in Fig. 3 for example, the same reaction time (*either* 100 ms *or* 300 ms, *depending upon the comparison*) was used and the same number of scans were taken to allow for a direct comparison between the spectra.

3. Results

3.1. Charge inversion using proteins as reagent ions

The tendency for proteins to form multiply charged ions via ESI is well known. Therefore, protein ions are plausible candidates for charge inversion reagents. Wells et al. reported reactions between oppositely charged protein ions that resulted in proton transfer and adduct formation but did not identify charge inversion products

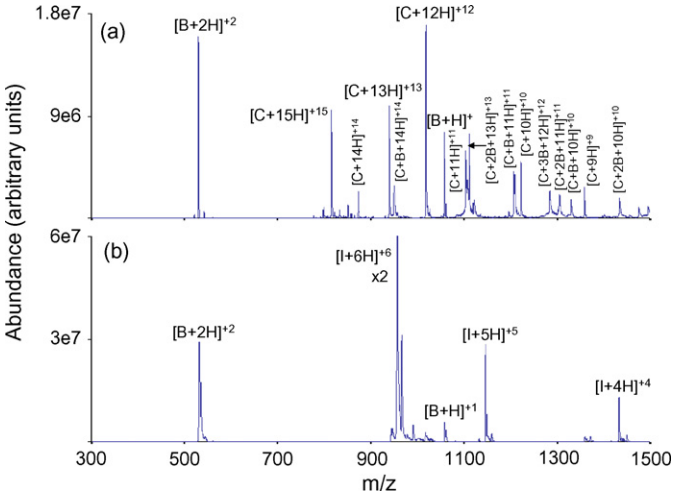

Fig. 1. (a) Post-ion/ion reaction spectrum of cytochrome *c* $[C+15]^{15+}$ ions with bradykinin $[B-H]^-$ ions; (b) post-ion/ion reaction spectrum of insulin $[I+6H]^{6+}$ ions with bradykinin $[B-H]^-$ ions.

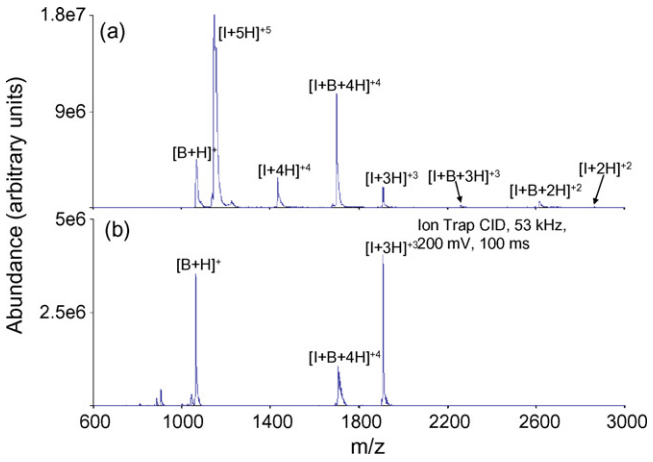

Fig. 2. (a) Post-ion/ion reaction spectrum of insulin $[I+5H]^{5+}$ with bradykinin $[B-H]^-$ anions (mass range extended by a factor of 2); (b) ion trap collision-induced dissociation of the $[I+B+4H]^{4+}$ complex (200 mV_{p-p}, 100 ms).

due to the fact that both the anions and cations were formed from the same protein [42]. To evaluate the utility of protein ions as charge inversion reagents, ion/ion reactions of deprotonated bradykinin (i.e., $[B-H]^-$) with multiply protonated cytochrome *c* ($[C+nH]^{n+}$) and multiply protonated insulin ($[I+nH]^{n+}$) were examined. The reactions resulted in the conversion of bradykinin from $[B-H]^-$ to $[B+H]^+$ and, for some reagents, to $[B+2H]^{2+}$, various extents of deprotonation of the protein ions, as well as attachment of bradykinin to cytochrome *c* and insulin, respectively. Fig. 1 shows results for $[C+15H]^{15+}$ (Fig. 1a) and $[I+6H]^{6+}$ (Fig. 1b). Contributions from both first and higher generation products, the latter of which are formed via sequential reactions, were noted in much of the data, particularly for the more highly charged reagents, due to the higher rates associated with the more highly charged protein cations [43].

The relative abundances of the bradykinin $[B+H]^+$ and $[B+2H]^{2+}$ ions differed significantly in the post-ion/ion reaction spectra for the different reagent cations. For example, both the $[C+15H]^{15+}$ and $[I+6H]^{6+}$ species showed relatively high tendencies for the transfer of three protons, thus giving rise to the $[B+2H]^{2+}$ product. Both give rise to +2:+1 bradykinin ion abundance ratios significant greater than 1, with the ratio resulting from the reaction with $[I+6H]^{6+}$ being the greatest of all of the reagents studied in this work. Clearly, the absolute charge of the reagent ion is not the sole or overriding factor in determining the +2:+1 bradykinin ion abundance ratio because the insulin ion carries fewer charges than does the cytochrome *c* ion. The number of protons that transfer from the reagent cations to the analyte anions is expected to be influenced by the numbers of basic sites in the reactants, the inherent basicities of those sites (i.e., in the absence of multiple charging), and the effect that electrostatic repulsion plays in altering the basicities of the sites due to multiple charging. This is highlighted in particular by the fact that the $[I+5H]^{5+}$ showed almost no tendency to transfer three protons to $[B-H]^-$ (see below). The dramatic difference in results for the insulin $[I+5H]^{5+}$ and $[I+6H]^{6+}$ ions highlights the important role that Coulomb repulsion can play in determining the partitioning of charge between the reactants [42].

Adduct species from both single and sequential ion/ion reactions are also often prominent in the data for the protein reagents, as is apparent in the $[C+15H]^{15+}$ data (see Fig. 1a) and in the $[I+5H]^{5+}$ data (see Fig. 2a). Note that the $[I+6H]^{6+}$ ion showed very little adduct formation when the mass range of the instrument was extended to scan over the range indicated in Fig. 2a (data not shown). The $[C+15H]^{15+}$ ion, with its greater charge, shows evidence for more sequential reactions than does the insulin $[I+5H]^{5+}$ ion under the conditions used here. For comparable reaction times and cation charge densities, such a result is expected due to the charge-squared rate dependence for ion/ion reactions. For example, cytochrome *c* ions with up to three bradykinin adducts are noted, whereas only one major adduct ion is observed for the insulin ions. Comparison of Figs. 1a and 2a also indicates that the fraction of ion/ion reactions that lead to adduct formation is lower for the $[C+15H]^{15+}$ reagent than for the $[I+5H]^{5+}$ ion. All ion/ion reactions that lead to charge inversion are expected to go through a relatively long-lived intermediate complex. The adduct ions are stabilized intermediates (see Section 4). The number of protons transferred to the analyte species is determined by the charge partitioning upon break-up of the complex. Collisional activation of the $[I+B+4H]^{4+}$ complex, for example, leads to the $[B+H]^+$ and $[I+3H]^{3+}$ ions as the dominant set of complementary fragment ions, as illustrated in Fig. 2b. It is noteworthy that essentially no $[I+4H]^{4+}$ signal is noted in the collision-induced dissociation of the complex, despite the appearance of a relatively abundant $[I+4H]^{4+}$ signal in the ion/ion reaction data (see Fig. 2a). Previous studies have suggested that single proton transfer reactions can take place via a curve crossing mechanism and need not proceed through a long-lived chemical complex (see Section 4). Evidence for single proton transfer reactions is also apparent in the data for the $[C+15H]^{15+}$ ion by the appearance of a relatively small signal for the $[C+14H]^{14+}$ species and in the $[I+6H]^{6+}$ data by the appearance of the $[I+5H]^{5+}$ signal. The charge inversion experiments involving protein cations as reagents clearly indicate that the tendencies for adduct formation and for transferring one, two, or three protons to deprotonated bradykinin are dependent upon charge as well as other characteristics of the ion, such as size and, perhaps, composition (e.g., numbers and exposures of basic, acidic, and other polar sites).

3.2. Charge inversion using DAB dendrimers

To investigate the effects of dendrimer size and charge state on charge inversion reactions, DAB dendrimer generations 1–5 were reacted with the bradykinin $[B-H]^-$ ion. The dendrimer cations represent reagents with much less variability than the protein reagents in that their surfaces are composed of primary amino groups. Hence, the comparison of two dendrimer ions of the same charge but different generation is more straightforward to make than, for example, a comparison between the same charge states of cytochrome *c* and insulin. None of the dendrimer ions, regardless

Table 1
Summary of charge inversion results of bradykinin $[B-H]^-$ from ion/ion reactions with generation 1–5 DAB dendrimers

Dendrimer generation	Bradykinin ratio: +2/+1
$[DAB_1+2H]^{2+}$	–
$[DAB_2+2H]^{2+}$	0
$[DAB_2+3H]^{3+}$	0
$[DAB_3+2H]^{2+}$	–
$[DAB_3+3H]^{3+}$	0
$[DAB_3+4H]^{4+}$	0
$[DAB_3+5H]^{5+}$	0.8
$[DAB_4+5H]^{5+}$	<0.1
$[DAB_4+6H]^{6+}$	2
$[DAB_4+7H]^{7+}$	2
$[DAB_5+7H]^{7+}$	1.3
$[DAB_5+8H]^{8+}$	2.8
$[DAB_5+9H]^{9+}$	3.0

The charge inversion ratio of bradykinin +2/+1 was calculated by dividing the absolute intensity of the bradykinin +2 ion by the absolute intensity of the bradykinin +1 ion in the post-ion/ion spectrum.

of generation or charge state, showed adduct formation with the bradykinin anion, which stands in contrast to the behavior noted with the protein cations, and also simplifies comparisons of +2:+1 bradykinin abundance ratios. For generations 3, 4, and 5, experiments were performed both on the 3D ion trap (multi-source instrument) and on a QTRAP 2000 instrument. For quantitative comparisons of bradykinin product ion abundance ratios, the QTRAP data are reported herein due to its superior reactant ion isolation capability. It was noted that the +2:+1 abundance ratios were sensitive to the number of DAB dendrimer reagent ions at long reagent ion accumulation times and/or high reagent signal levels in the mass spectrum. Specifically, the +2:+1 ratio could be increased dramatically by use of very high numbers of reagent ions. Data collected as a function of reagent ion accumulation time and with constant numbers of the bradykinin $[B-H]^-$ ions showed that the +1 ions were reduced at high reagent ion densities. This phenomenon is consistent with a space charge effect that discriminates against the $[B+H]^+$ ions. Under the constant storage conditions used in this work, the singly protonated bradykinin products are formed in a shallower trapping well than are the doubly protonated species. The singly charged ions are therefore more prone to loss from ion–ion repulsion, principally from the multiply charged dendrimer reagent ions present in high numbers. The ratios reported below, therefore, were collected under conditions in which they were insensitive to the number the reagent ions present (i.e., under conditions with minimal ion loss due to ion–ion repulsion). Table 1 summarizes the +2:+1 bradykinin abundance ratios obtained using the DAB dendrimer reagent ions studied here in the QTRAP instrument.

3.3. Dendrimer generation and charge state comparisons

No charge inversion was observed using the generation 1 $[DAB_1+2H]^{2+}$ dendrimer ion, and limited charge inversion was observed using generation 2 $[DAB_2+2H]^{2+}$ and $[DAB_2+3H]^{3+}$ ions. The latter ions produced low levels of $[B+H]^+$ ions upon reaction with $[B-H]^-$ but neither yielded readily measurable signals due to $[B+2H]^{2+}$ ions. The generation 3 dendrimer $[DAB_3+3H]^{3+}$, $[DAB_3+4H]^{4+}$, $[DAB_3+5H]^{5+}$ ions all converted at least some of the $[B-H]^-$ ions to $[B+H]^+$ whereas the $[DAB_3+2H]^{2+}$ ion gave rise to essentially no charge inversion of deprotonated bradykinin. Of the generation 3 ions studied, only the $[DAB_3+5H]^{5+}$ ion showed a tendency to yield significant abundances of both $[B+H]^+$ and $[B+2H]^{2+}$ ions. All of the DAB generation 4 and 5 ions studied, which carried net charges of +5 or greater, showed formation of both $[B+H]^+$ and $[B+2H]^{2+}$. For a given dendrimer generation, the general trend is to

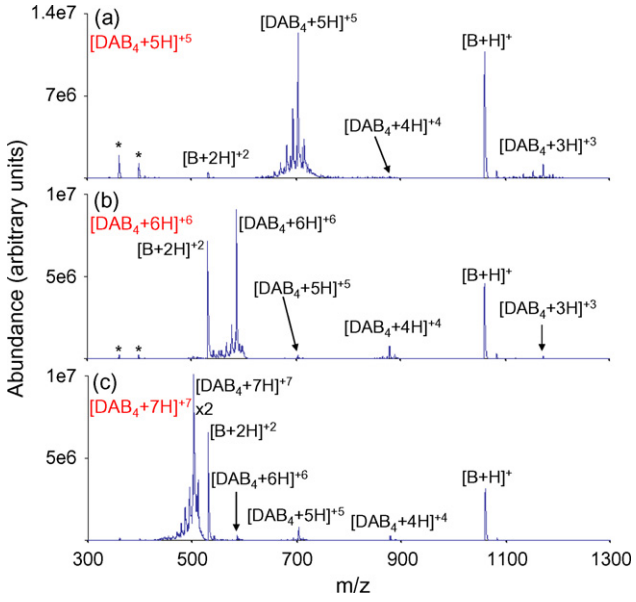

Fig. 3. Post-ion/ion reaction spectra from reaction of bradykinin $[B-H]^-$ ions with generation 4 DAB dendrimer ions (a) $[DAB_4+5H]^{5+}$, (b) $[DAB_4+6H]^{6+}$, and (c) $[DAB_4+7H]^{7+}$.

observe a higher propensity for charge inversion and higher +2:+1 abundance ratios as the charge state of the dendrimer increases. See Fig. 3, for example, which shows a comparison of data collected with the $[DAB_4+5H]^{5+}$, $[DAB_4+6H]^{6+}$, and $[DAB_4+7H]^{7+}$ ions. There is clearly a dramatic difference in going from $[DAB_4+5H]^{5+}$ to $[DAB_4+6H]^{6+}$, although the ratio does not change significantly from $[DAB_4+6H]^{6+}$ to $[DAB_4+7H]^{7+}$. There is a consistent trend in increasing +2:+1 bradykinin abundance ratios in the DAB_5 data.

For a given charge state, however, the size of the dendrimer is also expected to be a factor via its role in determining the electrostatic repulsion within the multiply charged ion. Higher charge densities are expected to lead to a greater tendency for the transfer of multiple protons. This data set tends to support this notion. A comparison of Fig. 3c with Fig. 4, which show data for the reaction of bradykinin $[B-H]^-$ with the +7 charge states of DAB generations 4 and 5, respectively, indicates that +2/+1 bradykinin abundance ratio from the smaller dendrimer (2) is larger than that formed from the larger dendrimer (1.3) of the same charge state. Such a result is consistent with a greater extent of proton transfer to bradykinin from dendrimer ions with greater electrostatic repulsion between the

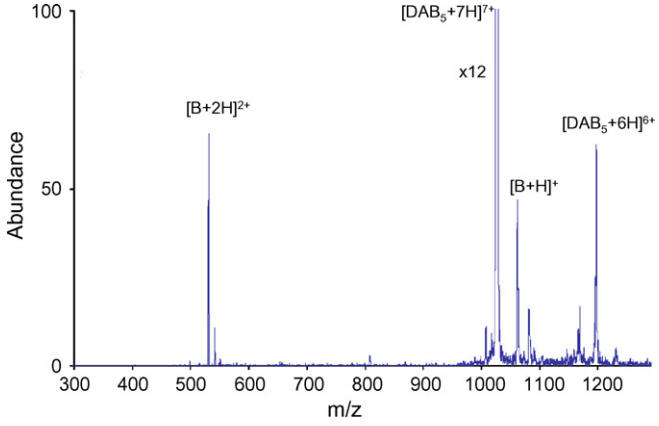

Fig. 4. Post-ion/ion reaction spectrum from the reaction of the bradykinin $[B-H]^-$ ion with the +7 charge state of DAB generation 5.

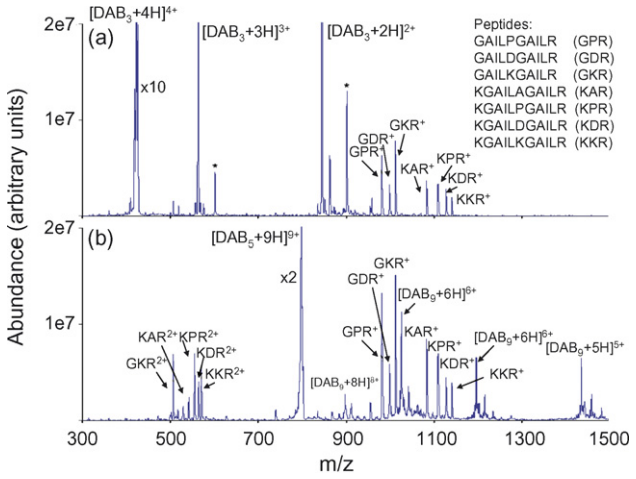

Fig. 5. The post-ion/ion reaction product ion spectrum of a mixture of singly deprotonated peptide anions using (a) $[DAB_3+4H]^{4+}$ as the reagent and (b) using $[DAB_5+9H]^{9+}$ as the reagent.

excess protons, as might be expected for the smaller dendrimer. A similar comparison for the +5 charge state ions derived from generations 3 and 4 show a similar tendency with the +2/+1 ratios being 0.8 and <0.1, respectively.

3.4. Charge inversion of a peptide mixture

The preceding results were obtained using a single peptide anion, deprotonated bradykinin, as a model and using the +2/+1 abundance ratio of the bradykinin products as a measure of the extent of proton transfer from a multiply protonated reagent. It is clear that the size and charge state of the reagent plays a major role in determining the extent of proton transfer to the peptide ion. We also examined a mixture of peptide ions comprised of a limited number of sequence differences to examine the role of peptide composition on the extent of proton transfer. Fig. 5 compares the post-ion/ion reaction data for the reaction of a mixture of deprotonated peptides comprised of the sequences GAILXGAILR (X = D, P, and K) and KGAILXGAILR (X = D, P, A, and K) with $[DAB_3+4H]^{4+}$ (Fig. 5a) and with $[DAB_5+9H]^{9+}$ (Fig. 5b). The data show that each of the peptides anions in the mixture underwent at least some charge inversion and also that the relative abundances of the singly protonated peptides formed via charge inversion are similar for both reagents. The greatest difference noted for the comparison of the two reagents is that essentially no doubly protonated peptides appear in the data for the $[DAB_3+4H]^{4+}$ reagent whereas five of the seven mixture components show some charge inversion to the doubly protonated species when $[DAB_5+9H]^{9+}$ serves as the reagent. All of the mixture components that are observed as doubly protonated species are comprised of at least two basic amino acids (i.e., all contain the C-terminal arginine and at least one lysine elsewhere in the peptide) as well as the N-terminus. Only the peptides lacking two basic amino acid side chains failed to yield doubly protonated species upon charge inversion. This set of data indicates at least some degree of selectivity in $-/n+$ charge inversion ion/ion reactions can be obtained with the appropriate selection of reagent cations. In this case, the $[DAB_5+9H]^{9+}$ reagent is capable of converting selectively to doubly protonated species those mixture components with at least two basic amino acids.

It is also of interest to compare the relative abundances of the charge inversion products of the peptide mixture components to the relative abundances of the deprotonated species subjected to ion/ion reactions. The relative signal levels associated with each peptide before (deprotonated peptide) and after (sum of signal due to singly and doubly protonated peptide) charge inversion is shown in Fig. 6 (normalized to the GAILKGAILR signal, which is the greatest of all mixture components in all spectra). The data for the $[DAB_3+4H]^{4+}$ reagent reflects fairly well the relative abundances of the singly protonated products derived from both reagents, as they were very similar. The relative abundances of the deprotonated peptides and protonated peptides do not show dramatic differences but it is clear that the cation signals do not reflect the anion signals with a high degree of fidelity. The mixture components that appear to undergo charge inversion least efficiently are those with an aspartic acid residue (i.e., KGAILDGAILR and GAILDGAILR). For these peptides, the relative abundance of the protonated species can be as little as half that of the corresponding deprotonated species. The difference in the overall cation relative abundances for the two reagents is largely due to the presence of doubly protonated mixture components in the case of the $[DAB_5+9H]^{9+}$ reagent, and the contributions of the doubly protonated species tends to increase the relative responses noted for those peptides with two or more basic amino acids. This data implies that acidic residues may decrease the charge inversion efficiency of peptides and that the amino acid composition of a peptide may play an important role in determining both the efficiency and the extent of charge inversion for a specific peptide.

4. Discussion

The conversion of a singly deprotonated molecule to a singly or multiply protonated molecule requires the transfer of two or

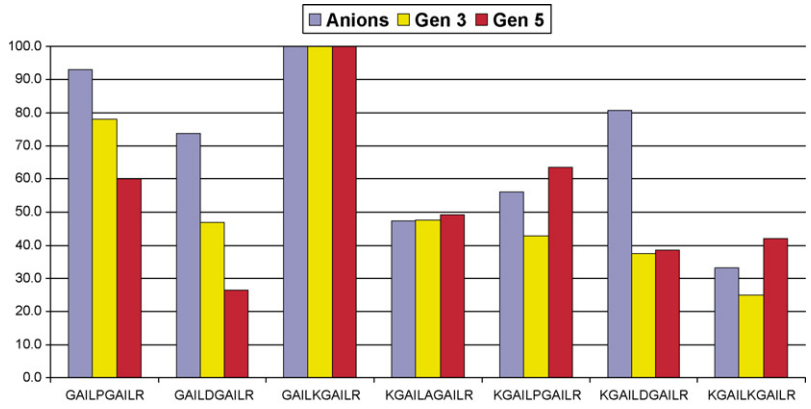

Fig. 6. Relative abundance of peptide anions prior to charge inversion (blue) and after charge inversion with generation 3 dendrimer cations (yellow) and generation 5 dendrimer cations (red).

more protons. It is highly unlikely that two or more successive proton transfer reactions will occur via sequential collisions under these reaction conditions due to the fact that the first proton transfer would form a neutral analyte molecule. The small absolute numbers of neutral analyte species formed by neutralization, coupled with the inherently low ion number densities in an ion trap, makes the probability for an ion/molecule collision involving a molecule formed by neutralization of an anion far too low to account for the observed signal levels. The formation of a multiply protonated molecule via a third consecutive proton transfer reaction is even less likely due to the repulsive interaction between the singly protonated analyte and the multiply protonated reagent. Therefore, the charge inversion products must arise from single ion/ion reaction encounters that give rise to an intermediate complex with a sufficient lifetime to allow for multiple proton transfers. Hence, the relative abundances of the charge inversion products are determined by how the intermediate analyte–reagent complex ion fragments.

The magnitudes and charge state dependencies of overall ion/ion reaction rates at or near thermal energy are consistent with the formation of an orbiting ion pair bound by the Coulombic attraction of oppositely charged reactants [42]. Previous studies involving reactions of multiply protonated proteins with multiply deprotonated proteins have suggested that after formation of the orbiting pair, two distinct proton transfer channels can be operative. One involves the formation of a long-lived "chemical" complex followed by dissociation of the complex, which is presumably the origin of the charge inversion products, and another involves charge transfer without the formation of a long-lived complex. The former process is analogous to ion/molecule proton transfer reactions at thermal energies that proceed through a long-lived intermediate [44]. The latter mechanism, referred to herein as "proton hopping", arises from the relatively high electric fields associated with oppositely charged ions as they approach each other and allows for proton transfer over distances sufficiently long to avoid formation of a complex [9]. The general kinetic scheme associated with the charge inversion of a singly deprotonated peptide, $[M-H]^-$, with a reagent with n excess protons, $[R+nH]^{n+}$, is shown in Scheme 1.

The scheme shows a rate constant for the formation of the ion/ion reaction pair, k_{pair}, which is the overall rate determining step. Ion trajectories within this orbiting pair are expected to be elliptical with varying degrees of eccentricity (a circular orbit represents a special case). Orbits that bring the ion pair sufficiently close for proton transfer but not close enough for a collision in which the partners come into intimate contact can lead to proton hopping and neutralization of the analyte. In this scheme the rate constant for proton hopping is represented by k_{hop}. The formation of a long-lived chemical intermediate is represented by the rate constant k_c. The intermediate can be stabilized via collisions and/or emission with an overall rate constant represented by k_{cool}, or it can dissociate into one of n proton transfer channels, represented by the various k_{diss} rate constants. The channel represented by $k_{diss}1$ reflects a single proton transfer to the analyte anion resulting in neutralization of the analyte. This process is experimentally indistinguishable from neutralization of the analyte via proton hopping. The other extreme, whereby all of the excess protons initially present on the reagent ion are transferred to M, thereby neutralizing the reagent, is represented by $k_{diss}n$. The channels represented by $k_{diss}1$ and $k_{diss}n$ share similar energy surfaces in that the products are comprised of an ion and a neutral species. All other dissociation channels represent cases in which both dissociation products are charged and are of like polarity. Such channels are characterized by a so-called Coulomb barrier [45], which can play a significant role in determining the rates of such reactions. One advantage to the product ions and the reagent ions being the same polarity is that further reaction of the reagent ions with the product ions is prevented. This indicates that charge inversion reactions could, in theory, have higher efficiencies than ion/ion reactions in which the desired product ions can react further with the reagent ions.

Two key figures of merit for a charge inversion reagent are the overall efficiency of conversion of the deprotonated analyte to analyte cations and the extent of charging in the charge inversion products, as reflected by the bradykinin +2/+1 abundance ratio in this study. Obviously, it is always desirable to maximize the overall efficiency but the desired extent of charging can be expected to be application dependent. A third figure of merit might be the extent of complex formation, although this can often be dealt with via subsequent activation of the complex to yield the desired analyte ions (for example, see Fig. 2b). The outcome of an ion/ion reaction reflected by Scheme 1, from which the figures of merit just described can be ascertained, is determined by the competition between proton hopping, which leads to analyte neutralization, and long-lived complex formation, which can lead to adduct formation, analyte neutralization, and/or charge inversion with varying extents of charging. To maximize overall efficiency, it is desirable to minimize the magnitude of k_{hop} relative to k_c and to minimize $k_{diss}1$ relative to the other k_{diss} values. For a given charge state, the magnitude of k_c is expected to increase relative to k_{hop} as the cross-section for a physical collision increases. This favors the use of relatively large reagents. Larger reagents may also reduce electrostatic repulsion within the reagent thereby reducing k_{hop}. However, increasing the size of the reagent for a given charge state may tend to decrease the extent of charging, as noted in the $[DAB_4+7H]^{7+}$ versus $[DAB_5+7H]^{7+}$ comparison.

The outcome of the pathway leading to long-lived complex formation determines the extent of charging and the tendency for

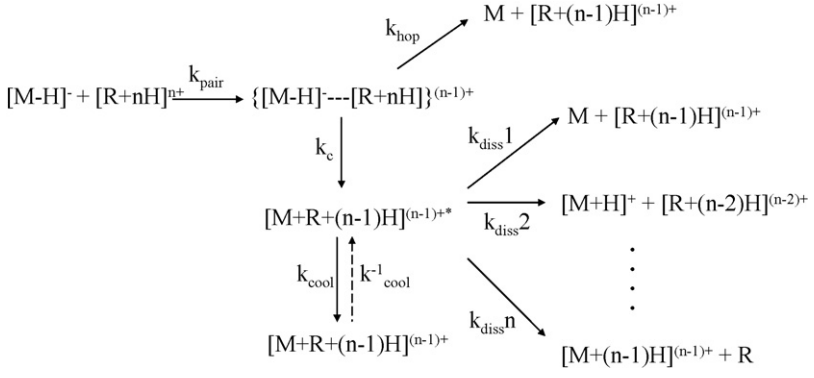

Scheme 1. Generic kinetic scheme for charge inversion of a singly deprotonated analyte, $[M-H]^-$, with a multiply protonated reagent, $[R+nH]^{n+}$.

observation of ion/ion attachment. The latter phenomenon is determined by the relative magnitudes of k_{cool} and the various k_{diss} values. The latter determine the lifetime of the ion/ion complex intermediate, the species indicated as $[M+R+(n-1)H]^{(n-1)+*}$. If the lifetime of the complex is sufficiently long to allow for collisional and radiative cooling to occur, ion/ion attachment, as frequently observed with the protein reagent ions (see above), can dominate. The relatively strong non-covalent interactions that can take place between polypeptides (e.g., interactions between acidic and basic side chains) tend to stabilize the complex with respect to dissociation and thereby maximize the likelihood for complex formation. The DAB dendrimers, on the other hand, with their monofunctionality at the surface apparently engage in weaker non-covalent interactions in the complex such that essentially none of the intermediate complexes appear in the post-ion/ion reaction product ion spectra.

With the exception of the single proton transfer channel characterized by $k_{diss}1$ in Scheme 1, the relative contributions of the competing dissociation channels from the complex are reflected in the extent of charging of the analyte. In this work, the most highly charged bradykinin ion was the +2 species, which is consistent with the presence of two strongly basic residues at each end of the nonapeptide. Hence, the only dissociation channels from break-up of the complex are those associated with one, two, or three proton transfers from the reagent. In the case of the doubly protonated reagents, only one and two proton transfers were possible. Hence, no dissociation channels involving charge separation were possible. It is interesting that neither the DAB_1 nor DAB_3 dications gave rise to measurable singly protonated bradykinin upon reaction with deprotonated bradykinin, whereas the corresponding DAB_2 dication did. This might be rationalized on the basis that the DAB_1 dendrimer, being relatively small, tended to neutralize deprotonated bradykinin via proton hopping with relatively little complex formation. The DAB_2 results indicate that at least some of the ion/ion interactions passed through a long-lived intermediate that would allow for two proton transfers. The fact that the DAB_3 ions, which would be expected to engage in more complex formation than the DAB_2 ions due to their larger collision cross-sections, did not give rise to measurable charge inversion suggests that single proton transfer (see the channel associated with $k_{diss}1$ in Scheme 1) dominates for the DAB_3 reagent whereas at least some two proton transfer reactions, leading to neutralization of the reagent, occurred with the DAB_2 dications. It might be expected that the DAB_3 dendrimer can better compete for the proton upon dissociation of the complex than can the DAB_2 dendrimer due to its greater number of basic sites and consequent ability to solvate and stabilize the proton.

For all dendrimer reagents with three or more excess charges, electrostatic repulsion between fragments of the complex and, in some cases, within fragments formed from the complex can play a significant role in determining the relative barriers to dissociation and thermodynamic stabilities of the products. All charge separation channels are characterized by a Coulomb barrier, but the relief of net electrostatic repulsion associated with separation of the fragments tends to favor such channels on a thermodynamic basis. This is increasingly true as the number of charges in the intermediate complex increases. Hence, the tendency for formation of doubly protonated bradykinin is expected, and is found, to increase with the total charge of the dendrimer. The extent of electrostatic repulsion in the reagent is expected to be a function both of net charge and of size. Hence, it might be expected that for a given charge state, smaller multiply protonated dendrimers might favor a greater extent of charging of the analyte upon charge inversion. The limited number of relevant comparisons forthcoming from this work appears to be consistent with this expectation.

5. Conclusions

Important characteristics of a reagent ion for charge inversion of singly deprotonated polypeptides include the extent of neutralization of the analyte ion, the magnitude of the positive charge that can be transferred to the polypeptide of interest, and the extent of ion/ion attachment. Multiply protonated proteins, which are readily formed over a range of charge states, can serve as charge inversion reagents but the formation of complexes is commonly observed. This is likely due to the potential for multiple and relatively strong non-covalent interactions between the protein reagent and the analyte polypeptide in long-lived proton transfer intermediate. As the protein charge state increases, the net charge of the intermediate also increases, which facilitates dissociation of the complex due to the relief of electrostatic repulsion. The smaller tendency for observation of complexes with high charge state reagents is consistent with this picture.

Multiply protonated amino-terminated dendrimers show no evidence for adduct formation in reactions with deprotonated bradykinin. Studies with ions over a range of charge states and over a range of dendrimer generations indicate that the extent of charging of bradykinin increases with the total charge of the dendrimer for a given generation. For a given charge state, the extent of proton transfer appears to be inversely related to dendrimer size. The extent of charging is interpreted as depending upon the outcome of the competition between various dissociation channels of a relatively long-lived intermediate within which proton transfer to the analyte from the dendrimer reagent can take place. The lack of adduct formation and the ability to form reagents with a range of charge states and from a range of generations makes amino-terminated dendrimers particularly attractive for inverting the charge of deprotonated polypeptides.

Acknowledgements

This work was supported by the Office of Basic Energy Sciences, Division of Chemical Sciences under Award No. DE-FG02-00ER15105. We acknowledge Dr. Min He and Dr. Harsha P. Gunawardena for their assistance with the four-source ITMS instrument and Dr. Yu Xia for helpful discussions during the preparation of this manuscript.

References

[1] M. Karas, F. Hillenkamp, Anal. Chem. 60 (1988) 2299.
[2] F. Hillenkamp, M. Karas, R.C. Beavis, B.T. Chait, Anal. Chem. 63 (1991) 1193A.
[3] J.B. Fenn, M. Mann, C.K. Meng, S.F. Wong, C.M. Whitehouse, Science 246 (1989) 64.
[4] A.R. Dongré, J.L. Jones, A. Somogyi, V.H. Wysocki, J. Am. Soc. Mass Spectrom. 118 (1996) 8365.
[5] M. He, G.E. Reid, H. Shang, G.U. Lee, S.A. McLuckey, Anal. Chem. 74 (2002) 4653.
[6] G.E. Reid, H. Shang, J.M. Hogan, G.U. Lee, S.A. McLuckey, J. Am. Chem. Soc. 124 (2002) 7353.
[7] G.E. Reid, J. Wu, P.A. Chrisman, J.M. Wells, S.A. McLuckey, Anal. Chem. 73 (2001) 3274.
[8] J.M. Hogan, S.A. McLuckey, J. Mass Spectrom. 38 (2003) 245.
[9] M. He, J.F. Emory, S.A. McLuckey, Anal. Chem. 77 (2005) 3173.
[10] D.C. Muddiman, X.H. Cheng, H.R. Udseth, R.D. Smith, J. Am. Soc. Mass Spectrom. 7 (1996) 697.
[11] S.A. McLuckey, G.J. Van Berkel, G.L. Glish, J. Am. Chem. Soc. 112 (1990) 5668.
[12] S.A. McLuckey, G.L. Glish, G.J. Van Berkel, Anal. Chem. 63 (1991) 1971.
[13] R.R.O. Loo, R.D. Smith, J. Mass Spectrom. 30 (1995) 339.
[14] R.A. Zubarev, D.M. Horn, E.K. Fridriksson, N.L. Kelleher, N.A. Kruger, M.A. Lewis, B.K. Carpenter, F.W. McLafferty, Anal. Chem. 72 (2000) 563.
[15] R.R.O. Loo, H.R. Udseth, R.D. Smith, J. Phys. Chem. 95 (1991) 6412.
[16] M. Scalf, M.S. Westphall, J. Krause, S.L. Kaufman, L.M. Smith, Science 283 (1999) 194.
[17] D.D. Ebeling, M.S. Westphall, M. Scalf, L.M. Smith, Anal. Chem. 72 (2000) 5158.
[18] J.L. Stephenson Jr., S.A. McLuckey, J. Am. Chem. Soc. 118 (1996) 7390.
[19] J.L. Stephenson Jr., S.A. McLuckey, Int. J. Mass Spectrom. Ion Process. 162 (1997) 89.

[20] J.M. Hogan, S.J. Pitteri, S.A. McLuckey, Anal. Chem. 75 (2003) 6509.
[21] J.L. Stephenson Jr., S.A. McLuckey, Anal. Chem. 68 (1996) 4026.
[22] J.L. Stephenson Jr., S.A. McLuckey, J. Am. Soc. Mass Spectrom. 9 (1998) 585.
[23] T.G. Schaaff, B.J. Cargile, J.L. Stephenson Jr., S.A. McLuckey, Anal. Chem. 72 (2000) 899.
[24] J.M. Wells, J.L. Stephenson, S.A. McLuckey, Int. J. Mass Spectrom. 203 (2000) A1.
[25] S.A. McLuckey, G.E. Reid, J.M. Wells, Anal. Chem. 74 (2002) 336.
[26] J.J. Coon, J.E.P. Syka, J.C. Schwartz, J. Shabanowitz, D.F. Hunt, Int. J. Mass Spectrom. 236 (2004) 33.
[27] P.A. Chrisman, S.J. Pitteri, J.M. Hogan, S.A. McLuckey, J. Am. Soc. Mass Spectrom. 16 (2005) 1020.
[28] R.G. Cooks (Ed.), Collision Spectroscopy, Plenum Press, New York, 1978.
[29] A.S. Danell, G.L. Glish, Int. J. Mass Spectrom. 212 (2001) 219.
[30] J.H. Bowie, T. Blumenthal, J. Am. Chem. Soc. 97 (1975) 2959.
[31] S. Hayakawa, Int. J. Mass Spectrom. 212 (2001) 229.
[32] M. He, S.A. McLuckey, Anal. Chem. 76 (2004) 4189.
[33] M. He, S.A. McLuckey, J. Am. Chem. Soc. 125 (2003) 7756.
[34] J.H. Bowie, C.S. Brinkworth, S. Dua, Mass Spectrom. Rev. 21 (2002) 87.
[35] H.P. Gunawardena, J.F. Emory, S.A. McLuckey, Anal. Chem. 78 (2006) 3788.
[36] X. Liang, H. Han, Y. Xia, S.A. McLuckey, J. Am. Soc. Mass Spectrom. 18 (2007) 369.
[37] E.R. Badman, P.A. Chrisman, S.A. McLuckey, Anal. Chem. 74 (2002) 6237.
[38] ICMS Software provided by N. Yates and the University of Florida.
[39] S.A. McLuckey, D.E. Goeringer, G.L. Glish, J. Am. Soc. Mass Spectrom. 2 (1991) 11.
[40] R.E. Kaiser Jr., R.G. Cooks, G.C. Stafford Jr., J.E.P. Syka, P.H. Hemberger, Int. J. Mass Spectrom. Ion Process. 106 (1991) 79.
[41] J.W. Hager, Rapid Commun. Mass Spectrom. 16 (2002) 512.
[42] J.M. Wells, P.A. Chrisman, S.A. McLuckey, J. Am. Chem. Soc. 125 (2003) 7238.
[43] S.A. McLuckey, J.L. Stephenson, K.G. Asano, Anal. Chem. 70 (1998) 1198.
[44] T. Su, M.T. Bowers, J. Am. Chem. Soc. 95 (1973) 7611.
[45] E.R. Williams, J. Mass Spectrom. 31 (1996) 831.